CrossMark

A comparative assessment of two kynurenic acid analogs in the formalin model of trigeminal activation: a behavioral, immunohistochemical and pharmacokinetic study

Gábor Veres[1,4] · Annamária Fejes-Szabó[1] · Dénes Zádori[1] · Gábor Nagy-Grócz[1,5] ·
Anna M. László[3] · Attila Bajtai[1] · István Mándity[2] · Márton Szentirmai[1] ·
Zsuzsanna Bohár[1,4] · Klaudia Laborc[1] · István Szatmári[2] · Ferenc Fülöp[2] ·
László Vécsei[1,4] · Árpád Párdutz[1]

Abstract Kynurenic acid (KYNA) has well-established protective properties against glutamatergic neurotransmission, which plays an essential role in the activation and sensitization process during some primary headache disorders. The goal of this study was to compare the effects of two KYNA analogs, N-(2-N,N-dimethylaminoethyl)-4-oxo-1H-quinoline-2-carboxamide hydrochloride (KA-1) and N-(2-N-pyrrolidinylethyl)-4-oxo-1H-quinoline-2-carboxamide hydrochloride (KA-2), in the orofacial formalin test of trigeminal pain. Following pretreatment with KA-1 or KA-2, rats were injected with subcutaneous formalin solution in the right whisker pad. Thereafter, the rubbing activity and c-Fos immunoreactivity changes in the spinal trigeminal nucleus pars caudalis (TNC) were investigated. To obtain pharmacokinetic data, KA-1, KA-2 and KYNA concentrations were measured following KA-1 or KA-2 injection. Behavioral tests demonstrated that KA-2 induced larger amelioration of formalin-evoked alterations as compared with KA-1 and the assessment of c-Fos immunoreactivity in the TNC yielded similar results. Although KA-1 treatment resulted in approximately four times larger area under the curve values in the serum relative to KA-2, the latter resulted in a higher KYNA elevation than in the case of KA-1. With regard to TNC, the concentration of KA-1 was under the limit of detection, while that of KA-2 was quite small and there was no major difference in the approximately tenfold KYNA elevations. These findings indicate that the differences between the beneficial effects of KA-1 and KA-2 may be explained by the markedly higher peripheral KYNA levels following KA-2 pretreatment. Targeting the peripheral component of trigeminal pain processing would provide an option for drug design which might prove beneficial in headache conditions.

Keywords Kynurenic acid analog · Rat · Trigeminal pain · Formalin test · Pharmacokinetics

G. Veres and A. Fejes-Szabó contributed equally to this work.

✉ László Vécsei
vecsei.laszlo@med.u-szeged.hu

1 Department of Neurology, Faculty of Medicine, Albert Szent-Györgyi Clinical Center, University of Szeged, Semmelweis u. 6, 6725 Szeged, Hungary

2 Institute of Pharmaceutical Chemistry, University of Szeged, Szeged, Hungary

3 Department of Biometrics and Agricultural Informatics, Faculty of Horticultural Science, Szent Istvan University, Budapest, Hungary

4 MTA-SZTE Neuroscience Research Group, Szeged, Hungary

5 Faculty of Health Sciences and Social Studies, University of Szeged, Szeged, Hungary

Introduction

The kynurenine pathway (KP) of the tryptophan (TRP) metabolism is extensively studied, mostly because of the well-established endogenous protective properties of kynurenic acid (KYNA) against the excitotoxic effect of other KP metabolites, such as quinolinic acid and 3-hydroxy-L-kynurenine (Vécsei et al. 2013; Zádori et al. 2011b). Thus, KYNA has become a molecule of interest for central nervous system (CNS) drug development for several disorders (Schwarcz 2004). The application of KYNA in in vivo preclinical studies would be difficult due to its chemical and pharmacokinetic properties. There are problems with its solubility in higher doses, it cannot pass the blood–brain barrier in an acceptable quantity and it has

Springer

a rapid clearance from the CNS and in the periphery, mediated by organic anion transporters (Bahn et al. 2005; Fukui et al. 1991). Several analogs, derivatives and prodrugs have been synthesized with the aim of mitigating these disadvantages and of improving the utility of the molecule in preclinical studies (Fülöp et al. 2009). Among our newly synthesized KYNA amides, two lead compounds have been identified (Patent number #P0900281/PCT/HU2010/00050).

With regard to in vitro electrophysiology studies, *N*-(2-*N*,*N*-dimethylaminoethyl)-4-oxo-1H-quinoline-2-carboxamide hydrochloride (KA-1, Fig. 1a) has been demonstrated to be an even more effective inhibitor of hippocampal excitatory synaptic transmission than KYNA (Nagy et al. 2011). Accordingly, in an in vivo model of trigeminal activation, KA-1 displayed better efficacy than that of its parent compound, KYNA (Knyihár-Csillik et al. 2008). Following this comparative study, KA-1 was tested in several experimental setups and proved to have beneficial effects (Gellért et al. 2012, 2011; Knyihár-Csillik et al. 2008; Marosi et al. 2010; Vámos et al. 2010, 2009; Zádori et al. 2011c). In contrast with the electrophysiological findings with KA-1, *N*-(2-*N*-pyrrolidinylethyl)-4-oxo-1H-quinoline-2-carboxamide hydrochloride (KA-2, Fig. 1b) did not decrease, but rather slightly increased the amplitudes of field excitatory postsynaptic potentials (fEPSPs) (Nagy et al. 2011). However, in a recent study, pretreatment with KA-2 was also able to attenuate the effects of nitroglycerine (NTG) in an experimental model of migraine (Fejes-Szabó et al. 2014).

The modes of action of these two compounds are still not fully understood. The two main possibilities are the following: (1) the intact structure is necessary for the mechanism of action, which would mimic some effects of the parent compound, KYNA; (2) the KYNA amides serve as prodrugs and dissociate into KYNA, which can exert its

pharmacological effects. With regard to the clarification of this issue, only one pharmacokinetic study is available to date (Zádori et al. 2011a). In that study, KYNA and KA-1 levels were measured with high-performance liquid chromatography (HPLC) in C57B/6 mouse serum following the intraperitoneal administration of KA-1. The time-course profile of KA-1 exhibited a steep increase in concentration followed by a rapid decrease in the first hour. Although the concentration of KYNA also increased from the basal serum level following KA-1 administration, this increase was considerably less than that in the case of KA-1. It may therefore be concluded that only a small proportion of KA-1 is metabolized to KYNA. These findings and the results of electrophysiology studies led to the assumption that it is less likely that KA-1 acts as a prodrug. Similar pharmacokinetic studies relating to KA-2 have not yet been made, but in view of the results of the electrophysiology studies, it seems to have a different mode of action.

The trigeminal system is responsible for most of the pain processing originating from the area of the head (Carpenter and Sutin 1983), and its activation therefore plays an important role in the pathomechanism of several neurological disorders, including primary headaches and trigeminal pain syndromes. These disorders, including migraine cause an enormous burden to the society (Olesen et al. 2012) underlining the need of new treatment options with a possible different mechanism of action. On the basis of its antagonistic influence on *N*-methyl-D-aspartate (NMDA), α-amino-3-hydroxy-5-methyl-4-isoxazolepropionic acid (AMPA) and kainate receptors (Pereira et al. 2002), it is assumed that KYNA has a modifying effect on nociception (Näsström et al. 1992; Párdutz et al. 2012), and thus might possibly be a future candidate in headache treatment.

One aim of this study was to investigate the effects of KA-1 and KA-2 in the orofacial formalin test to quantify the nociception in the trigeminal region of the rat (Clavelou et al. 1995; Raboisson and Dallel 2004). A further aim was to perform a comparative pharmacokinetic study so as to further clarify the possible modes of action of these two KYNA amides.

Materials and methods

Animals

During the experiments, adult male Sprague–Dawley rats weighing 200–250 g were used. The animals were housed under standard laboratory conditions (in an air-conditioned, humidity-controlled and ventilated room) and were allowed free access to drinking water and regular rat chow on a 12 h–12 h dark–light cycle. The procedures used in
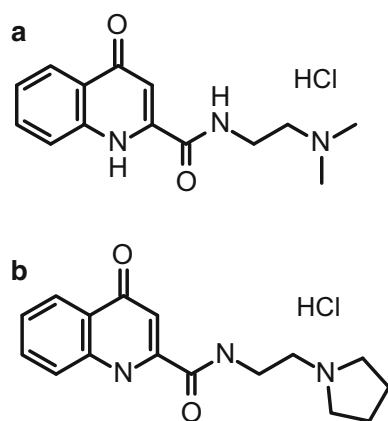

Fig. 1 The chemical structure of *N*-(2-*N*,*N*-dimethylaminoethyl)-4-oxo-1H-quinoline-2-carboxamide hydrochloride (KA-1, **a**) and *N*-(2-*N*-pyrrolidinylethyl)-4-oxo-1H-quinoline-2-carboxamide hydrochloride (KA-2, **b**)

this study followed the guidelines of the International Association for the Study of Pain and the directive of the European Economic Community (86/609/ECC). They were approved by the Committee of Animal Research at the University of Szeged (I-74-12/2012) and the Scientific Ethics Committee for Animal Research of the Protection of Animals Advisory Board (XXIV./352/2012.).

Materials

The new KYNA amides (patent number #P0900281/PCT/HU2010/00050), KA-1 and KA-2, were synthesized in the Department of Pharmaceutical Chemistry, University of Szeged. The reference compounds [KYNA and 3-nitro-L-tyrosine (3-NLT)], zinc acetate dihydrate, chloral hydrate and 3,3′-diaminobenzidine were purchased from Sigma-Aldrich (Saint Louis, MO, USA), acetonitrile, H_2O_2, nickel ammonium sulfate and perchloric acid (PCA) were purchased from Scharlau (Barcelona, Spain), acetic acid and Triton X-100 were purchased from VWR International (Radnar, PA, USA), and paraformaldehyde was purchased from Merck (Darmstadt, Germany). The HPLC–MS grade acetonitrile and acetic acid were obtained from VWR International (Radnar, PA, USA).

Behavioral testing

To produce and quantify nociception in the trigeminal region of the rat, we used the orofacial formalin test.

The animals were divided into three groups ($n = 27$–28 per group) and received an intraperitoneal (i.p.) injection of phosphate-buffered saline (PBS, 0.1 M, pH 7.4) in the Control group or an i.p. injection of KA-1 (1 mmol/kg body weight; pH 7.4) in the KA-1 group or an i.p. injection of KA-2 (1 mmol/kg body weight; pH 7.4) in the KA-2 group. One hour after pretreatment, the animals were divided further into two subgroups ($n = 13$–15 per subgroup), half of the rats receiving a subcutaneous (s.c.) injection of 50 μl physiological saline without formalin (control, KA-1 and KA-2), while the other half of the rats were injected s.c. with 50 μl 1.5 % formalin solution containing 0.55 % formaldehyde (control–formalin, KA-1–formalin and KA-2–formalin), administered via a 26-gauge needle into the right whisker pad.

The testing procedures were performed during the light phase (between 8 a.m. and 2 p.m.) in a quiet room. The test box was a 30 × 30 × 30 cm glass terrarium with mirrored walls. For the offline analysis of rubbing activity directed to the whisker pad, the behavior of the individually tested rats was recorded with a video camera (Logitech HD Webcam C615) situated 1 m above the terrarium. One hour after pretreatment and following a 10-min habituation period in the test box, the whisker pads of the rats were injected s.c. with physiological saline or formalin and the animals were immediately replaced in the chamber for 45-min. The rats did not receive any food or water during the observation period. The test box was cleaned and decontaminated after each animal. An observer blind to the experimental procedures analyzed the recorded videos. The 45-min recording period was divided into 15 × 3-min blocks, and we distinguished two phases following formalin injection [Phase 1 (time block 1, i.e., 0–3 min) and Phase 2 (time blocks 5–15, i.e., 12–45 min)] according to the previously published methods (Clavelou et al. 1995; Raboisson and Dallel 2004), and the total time (number of seconds) spent in rubbing/scraping the injected area with the ipsilateral fore- or hindpaw was measured in each block and defined as the nociceptive score for that block. Earlier literature findings led us to use the grooming activity of animals in the control subgroup as control (Clavelou et al. 1995).

Immunohistochemistry

Four hours after the formalin injection, the rats were perfused transcardially with 100 ml PBS, followed by 500 ml 4 % paraformaldehyde in phosphate buffer under deep chloral hydrate (0.4 g/kg body weight) anesthesia. The medullary segment containing the spinal trigeminal nucleus pars caudalis (TNC) between +1 and −5 mm from the obex was removed, postfixed overnight for immunohistochemistry in the same fixative and cryoprotected (10 % sucrose for 2 h, 20 % sucrose until the blocks sank, and 30 % sucrose overnight). Before sectioning, each segment was marked with a small incision on the ventral and left (contralateral) side of the tissue block, allowing side discrimination during the quantification process. 30-μm transverse cryostat sections were cut through the rostrocaudal axis from the beginning of the TNC and were serially collected in wells containing cold PBS. Each well contained every tenth section at 0.3-mm intervals along the rostrocaudal axis (15 levels = sections). The free-floating sections were rinsed in PBS and immersed in 0.3 % H_2O_2 in PBS for 30 min to suppress endogenous peroxidase activity. After several rinses in PBS containing 1 % Triton X-100 (PBST), sections were incubated at room temperature overnight in PBST containing rabbit anti-rat c-Fos polyclonal antibody (Santa Cruz Biotechnology, sc-52) at a dilution of 1:2000. The immunohistochemical reaction was visualized using Vectastain Elite avidin–biotin kits (Vector Laboratories, PK6101). Briefly, the sections were incubated at room temperature for 2 h in PBST containing goat anti-rabbit biotinylated secondary antibody. After several rinses in PBST, and incubation at room temperature for 2 h in PBST containing avidin and biotinylated horseradish peroxidase, the sections were stained with 3,3′-

diaminobenzidine intensified with nickel ammonium sulfate. The specificity of the immune reactions was checked by omitting the primary antiserum.

The immunoreactive (IR) cells in the superficial layer of the TNC were counted by an observer blind to the experimental procedures under the $10\times$ objective of a Nikon Optiphot-2 (Nikon Instruments, Melville, NY, USA) light microscope in every tenth transverse section in each animal. Before the counting, the location of each section along the rostrocaudal axis and the location of the TNC on each medullary section were determined by means of The Rat Brain in Stereotaxic Coordinates Atlas (Paxinos and Watson 2007). The c-Fos neurons with obvious specific nuclear staining were taken into consideration and were counted in the TNC both ipsilaterally and contralaterally to the formalin injection.

HPLC measurements

Sample preparation

At set time points (15, 30, 60, 120 and 300 min) following the i.p. injection with the KYNA amides (1 mmol/kg), the rats were deeply anesthetized with i.p. injection of chloral hydrate (0.4 g/kg, Sigma-Aldrich). Blood samples were collected from vena cava caudalis and centrifuged at 13709 RCF (relative centrifugal force) for 10 min at 4 °C. The supernatants, i.e., the serum samples, were collected and centrifuged at 13709 RCF for 10 min at 4 °C again and the supernatants were stored at −80 °C until use. After the collection of blood samples, the animals were transcardially perfused with 100 ml 0.1 M PBS for 5 min. The CNS samples containing the medullary segment of the TNC were then removed and stored at −80 °C until measurements. The animals in the Control group underwent a similar procedure with one measurement point at 300 min.

For the measurement of KYNA concentration, the CNS samples were cut in half, weighed and then sonicated for 1.5 min in an ice-cooled solution (250 μl) comprising PCA (2.5 % w/w), 3-NLT (10 or 2 μM) and distilled water in an Eppendorf tube. The content of the Eppendorf tube was centrifuged at 13709 RCF for 10 min at 4 °C and the supernatant was measured. Before analysis, the serum samples were thawed and, after a brief vortex, the serum sample was 'shot' onto a precipitation solvent (containing PCA with 3-NLT as internal standard, with resulting concentrations of 2.5 w/w% and 2 μM, respectively). The samples were subsequently centrifuged at 13709 RCF for 10 min at 4 °C, and the supernatants were collected for measurement.

For the analysis of KYNA amides, the other half of the CNS samples were weighed and then sonicated in ice-cold (250 μl) distilled water for 1.5 min and centrifuged at

13709 RCF for 10 min at 4 °C. From the supernatant, 100 μl was transferred to an Eppendorf tube containing 750 μl HPLC gradient grade acetonitrile and 150 μl distilled water. After a brief vortex, the samples were centrifuged at 13709 RCF for 10 min at 4 °C and 900 μl of supernatant was evaporated in a vacuum centrifuge. After thawing and brief stirring with a vortex, 200 μl of serum sample was transferred to an Eppendorf tube containing 700 μl HPLC gradient grade acetonitrile and 100 μl distilled water. After a brief vortex, the samples were centrifuged at 13709 RCF for 10 min at 4 °C and 900 μl of supernatant was evaporated in a vacuum centrifuge. The evaporated CNS and serum samples were stored at 4 °C until use.

Chromatographic conditions

The KYNA concentrations of the CNS samples were quantified on the basis of a slight modification of a literature method (Hervé et al. 1996) as described in detail with method validation in our previous article (Fejes-Szabó et al. 2014). For the measurement of concentration of the above-mentioned metabolite from serum samples we applied the same method with a slight modification. Furthermore, we applied the method validation procedures to the serum samples too. Briefly, we used an Agilent 1100 HPLC system (Agilent Technologies, Santa Clara, CA, USA) equipped with fluorescence and a UV detector; the former was applied for the determination of KYNA and the latter for the determination of the internal standard (3-NLT). Chromatographic separations were performed on an Onyx Monolithic C18 column, 100 mm × 4.6 mm I.D. (Phenomenex Inc., Torrance, CA, USA) after passage through a SecurityGuard pre-column C18, 4 × 3.0 mm I.D., 5 μm particle size (Phenomenex Inc., Torrance, CA, USA) with a mobile phase composition of 0.2 M zinc acetate/ACN = 95/5 (v/v), the pH of which was adjusted to 6.2 with acetic acid, applying isocratic elution. The flow rate was 1.5 ml/min and the injection volume was 20 μl for serum, and 50 μl for CNS samples. The fluorescence detector was set at excitation and emission wavelengths of 344 and 398 nm. The UV detector was set at a wavelength of 365 nm.

For the determination of KYNA amides, a Thermo LCQFleet ion trap mass spectrometer was used equipped with an ESI ion source combined with a Dionex Ultimate 3000 HPLC system. The ionization parameters were as follows: heater temperature: 500 °C, sheath gas flow rate: 60, auxiliary gas flow rate: 20, spray voltage: 4 kV, capillary temperature: 400 °C. Chromatographic separations were performed on a Kinetex C18 column, 100 mm × 4.6 mm, 2.6 μm particle size (Phenomenex Inc., Torrance, CA, USA) after passage through a SecurityGuard pre-

column C18, 4×3.0 mm, 5 μm particle size (Phenomenex Inc., Torrance, CA, USA), with a mobile phase composition of 0.05 % aqueous CH_3COOH/ACN = 90/10 (v/v), applying isocratic elution. The flow rate and the injection volume were 1 ml/min and 50 μl, respectively.

Calibration curve and linearity

Calibrants were prepared at six different concentration levels, from 1 to 100 nM, 0.5 to 5 μM and 0.01 to 100 μM for KYNA, 3-NLT and the KYNA amides, respectively. Three parallel injections of each solution were made under the chromatographic conditions described above. The peak area responses were plotted against the corresponding concentration, and the linear regression computations were carried out by the least square method with the freely available R software (R Development Core Team 2002). Very good linearity was observed throughout the investigated concentration ranges for KYNA, 3-NLT and the

KYNA amides when either fluorescence, UV or MS detection was applied.

Selectivity

The selectivity of the method was checked by comparing the chromatograms of KYNA, KYNA amides and the internal standard for a blank serum and CNS sample and those for a spiked sample. All compounds could be detected in their own selected chromatograms without any significant interference.

LOD and LLOQ

The limit of detection (LOD) and the lower limit of quantification (LLOQ) were determined via the signal-to-noise ratio with a threshold of 3 and 10, respectively, according to the ICH guidelines (ICH 1995). The LOD and LLOQ for KYNA in the serum samples were 1 and
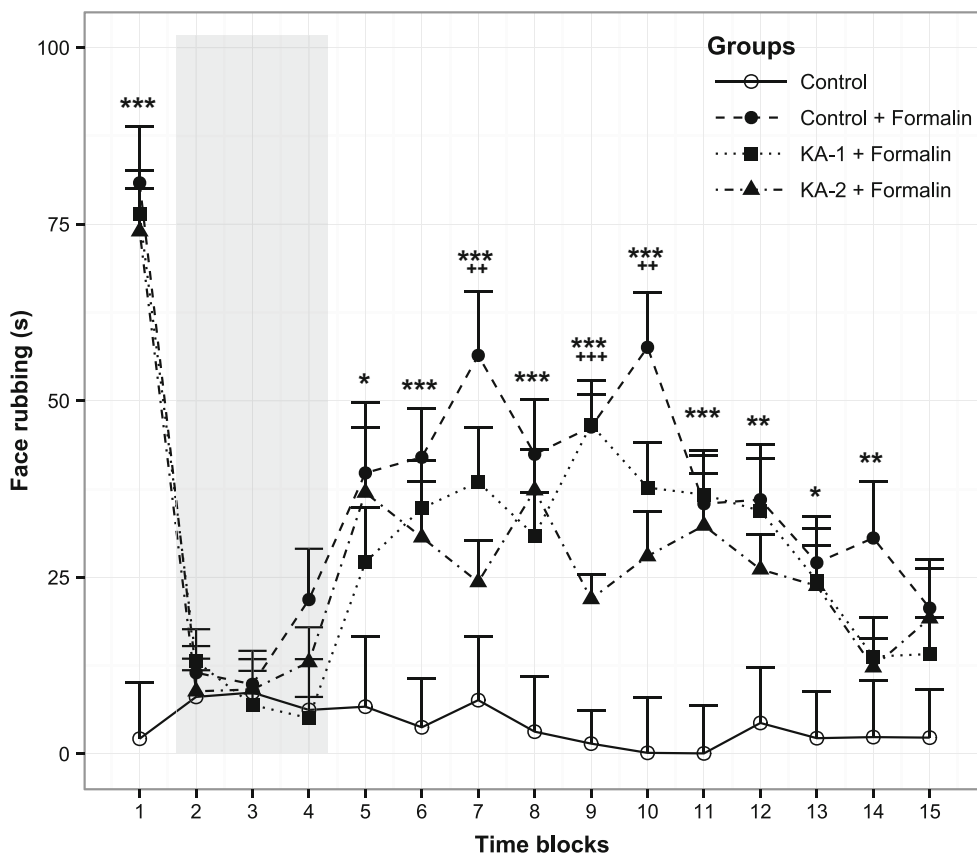

Fig. 2 The effects of formalin and KYNA amide treatments on Sprague–Dawley male rats in the orofacial formalin tests. Following formalin injection, the recording period was 45-min and this time period was divided into 15×3-min time blocks. Phase 1 (time block 1) of the test is before the grayed out area, while Phase 2 (time blocks 5–15) is after the grayed out area. The two phases of formalin action in the control + formalin group are well demonstrated when compared to the control group ($*p < 0.05$; $**p < 0.01$; $***p < 0.001$).

The KA-2 pretreatment significantly reduced the formalin-induced nociceptive behavior relative to the control + formalin group ($^{++}p < 0.01$; $^{+++}p < 0.001$). Sprague–Dawley male rats: $n = 13$–15 in each group; data are shown as mean ± SEM; *KA-1* N-(2-N,N-dimethylaminoethyl)-4-oxo-1H-quinoline-2-carboxamide hydrochloride; *KA-2* N-(2-N-pyrrolidinylethyl)-4-oxo-1H-quinoline-2-carboxamide hydrochloride
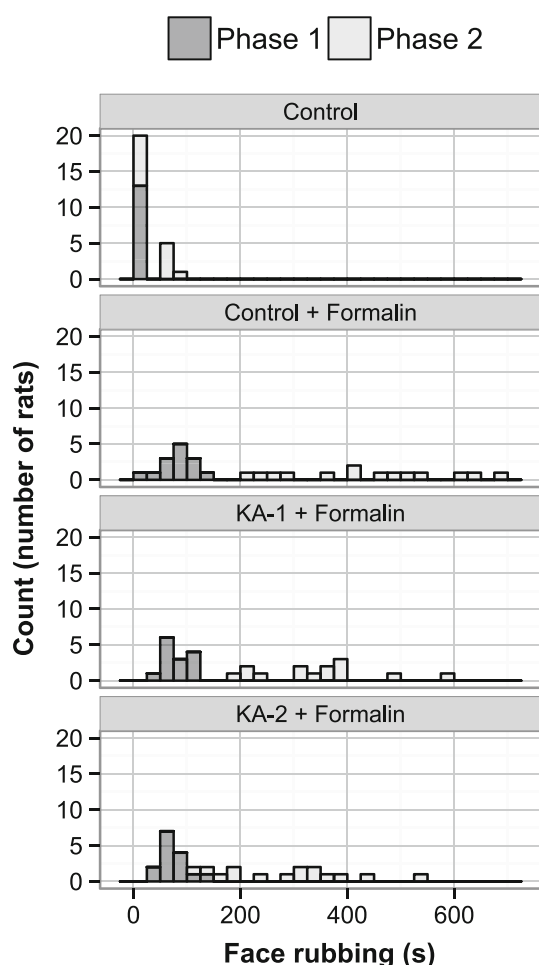
Fig. 3 Distribution of rubbing activity by groups in Phase 1 and 2 of the orofacial formalin test. The recording period was 45-min, Phase 1 is the first 3-min, while Phase 2 is the overall rubbing activity from min 12 to the end of the examination. Sprague–Dawley male rats: $n = 13$–15 in each group; *KA-1 N*-(2-*N*,*N*-dimethylaminoethyl)-4-oxo-1H-quinoline-2-carboxamide hydrochloride; *KA-2 N*-(2-*N*-pyrrolidinylethyl)-4-oxo-1H-quinoline-2-carboxamide hydrochloride

3.75 nM, respectively, while in the CNS samples they were 0.4 and 1 nM, respectively. The LOD and LLOQ for the samples in MS detection were 0.001 and 0.015 μM, respectively.

Precision

Replicate HPLC analysis showed that the relative standard deviation was $\leq 2.2\%$ for the peak area response and $\leq 0.1\%$ for the retention time for KYNA and the KYNA amides.

Recovery

The relative recoveries were estimated by measuring spiked samples of KYNA and the KYNA amides at two concentrations with three replicates of each. No significant

differences were observed for the lower and higher concentrations. The recoveries for the serum samples ranged from 103 to 108 %, 81 to 94 % and 79 to 80 % for KYNA, KA-1 and KA-2, respectively. The recoveries for the CNS samples ranged from 82 to 92 % and 78 to 84 % for KYNA and KA-2, respectively.

Data evaluation

To compare the means of jaw rubbing counts (orofacial formalin tests) in the different treatment groups (control, control–formalin, KA-1, KA-1–formalin, KA-2, KA-2–formalin) on rats during 15 3-min time periods ($n = 13$–15 animals in each group), two-way repeated measures ANOVA were run. Treatment with six groups was used as between-subject factor and time with 15 time points as within-subject factor for the analysis.

When Levene's test for homogeneity of variance was significant in the Phase data (Phase 1 is the first 3 min, while Phase 2 is the overall rubbing from min 12 to the end of the examination, min 45, i.e., which is from the fifth 3-min time period to the 15th), the Welch test was run to compare mean rubbing counts. Pairwise comparisons were estimated by the Sidak test. The effect size (EF, f) was calculated according to Cohen J. (Cohen 1988) with regard to the ANOVA tests comparing the effects of compounds on behavioral data in Phase 1 and 2.

In the case of the immunohistochemistry data, the numbers of c-Fos-containing nuclei were assessed. Three-way repeated measures ANOVA was used to analyze group means across 15 adjacent measuring sites (consequent slices from the medullary segment of the CNS containing the TNC) among sides (contralateral and ipsilateral) and between pretreatment groups (control, KA-1 and KA-2) all with formalin injections. Measuring sites and sides were used as within-subject factor, while pretreatment was the between-subject factor in the general linear model.

In the ANOVA models when Mauchly's test of sphericity was significant, the Greenhouse–Geisser correction was performed. In the event of the significant interaction of factors, effects could not be reported independently. Moreover, owing to the significant interaction, group differences could be examined separately over the within-subject factor based on estimated marginal means for multiple comparisons with the Sidak adjustment.

Statistical analyses were carried out with IBM SPSS Statistics, version 21 (IBM Corporation, Armonk, NY, USA) software. All tests were two-sided, and $p < 0.05$ was considered to be statistically significant. The pharmacokinetic data were evaluated with PKSolver, a freely available menu-driven add-in program for Microsoft Excel (Zhang et al. 2010).

Fig. 4 Diagrams showing the rubbing activity in the first (**a**) and the second (**b**) phase in the orofacial formalin test. In the control + formalin group, the subcutaneous formalin injection induced a significant increase in rubbing activity in both Phase 1 and 2 (***$p < 0.001$) as compared to the control group. In Phase 2, pretreatment with KA-2 had a significant effect on mitigating the formalin-induced increase in the time spent with rubbing (++$p < 0.01$) as compared with the control + formalin group. Sprague–Dawley male rats: $n = 13$–15 in each group; data are presented as mean ± SEM; *KA-1* N-(2-N,N-dimethylaminoethyl)-4-oxo-1H-quinoline-2-carboxamide hydrochloride; *KA-2* N-(2-N-pyrrolidinylethyl)-4-oxo-1H-quinoline-2-carboxamide hydrochloride
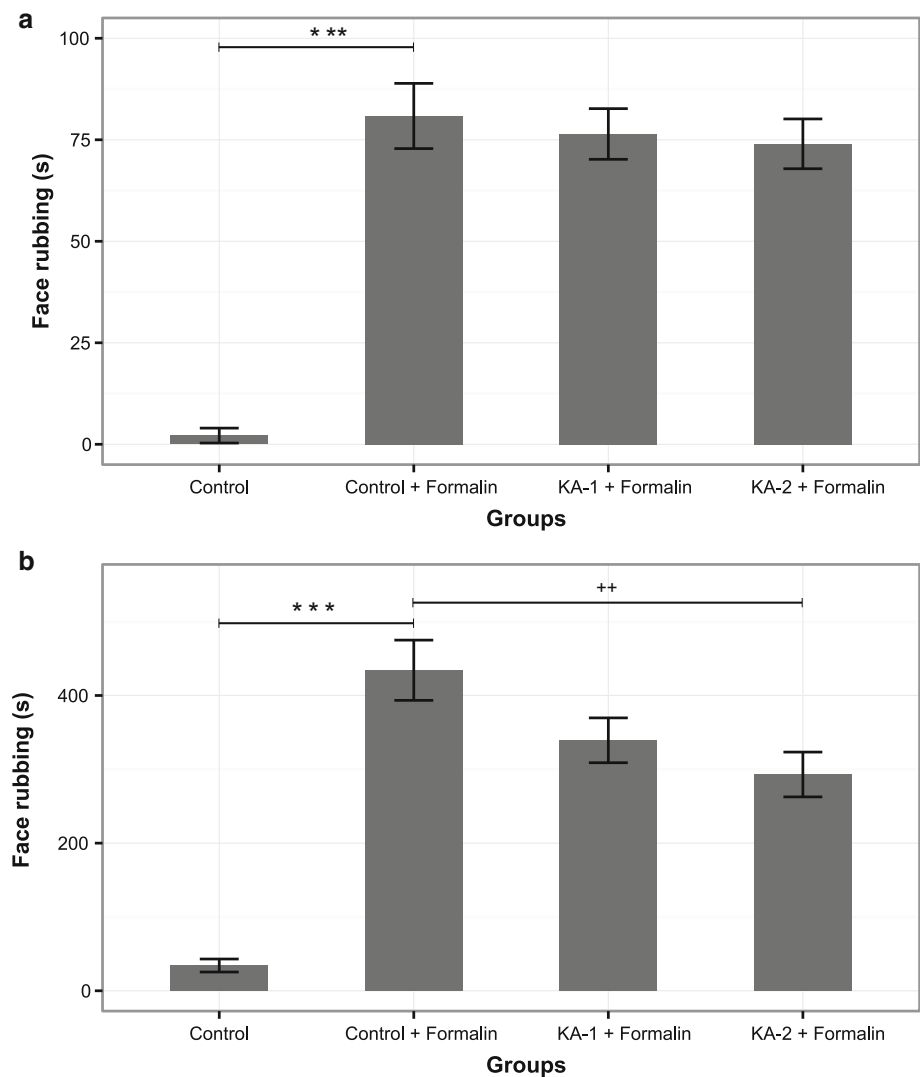
Results

Behavioral assessment

The results of orofacial formalin testing are demonstrated in Figs. 2, 3 and 4. To simplify the presentation of group comparisons for better transparency, the groups of KA-1 and KA-2 were omitted from Figs. 2, 3 and 4. Pairwise comparisons revealed that face rubbing activity in the control, KA-1 and in the KA-2-treated groups was significantly lower in both Phase 1 and Phase 2 compared with the control–formalin (ES of Phase 1, −1.88 and Phase 2, −2.17), KA-1–formalin (ES of Phase 1, −1.75 and Phase 2, −1.56) and KA-2–formalin (ES of Phase 1, −1.64 and Phase 2, −1.26) groups. With regard to the comparison of the face rubbing activity in the KA-1–formalin (ES of Phase 1, 0.11 and Phase 2, 0.51) and KA-2–formalin (ES of Phase 1: 0.16 and Phase 2: 0.76) groups with that in the control–formalin group, although KA-1 decreased face

rubbing activity as well (demonstrated by the corresponding left-skewed histogram in Fig. 3), only KA-2 treatment resulted in a significant reduction in the middle of Phase 2 (Figs. 2, 4).

Immunohistochemistry

The results of immunohistochemical analysis are demonstrated in Figs. 5 and 6. The comparison of the ipsilateral and the contralateral sides of the slices from the medullary segment of the rat CNS containing the TNC demonstrated that the mean number of c-Fos IR neurons was significantly higher on the ipsilateral side than on the contralateral side in the control–formalin, KA-1–formalin and KA-2–formalin groups (the two latter groups are not demonstrated to simplify the presentation of group comparisons for better transparency in Fig. 6). With regard to the comparison of the ipsilateral sides of the KA-1–formalin and KA-2–formalin groups with the control–formalin group from the
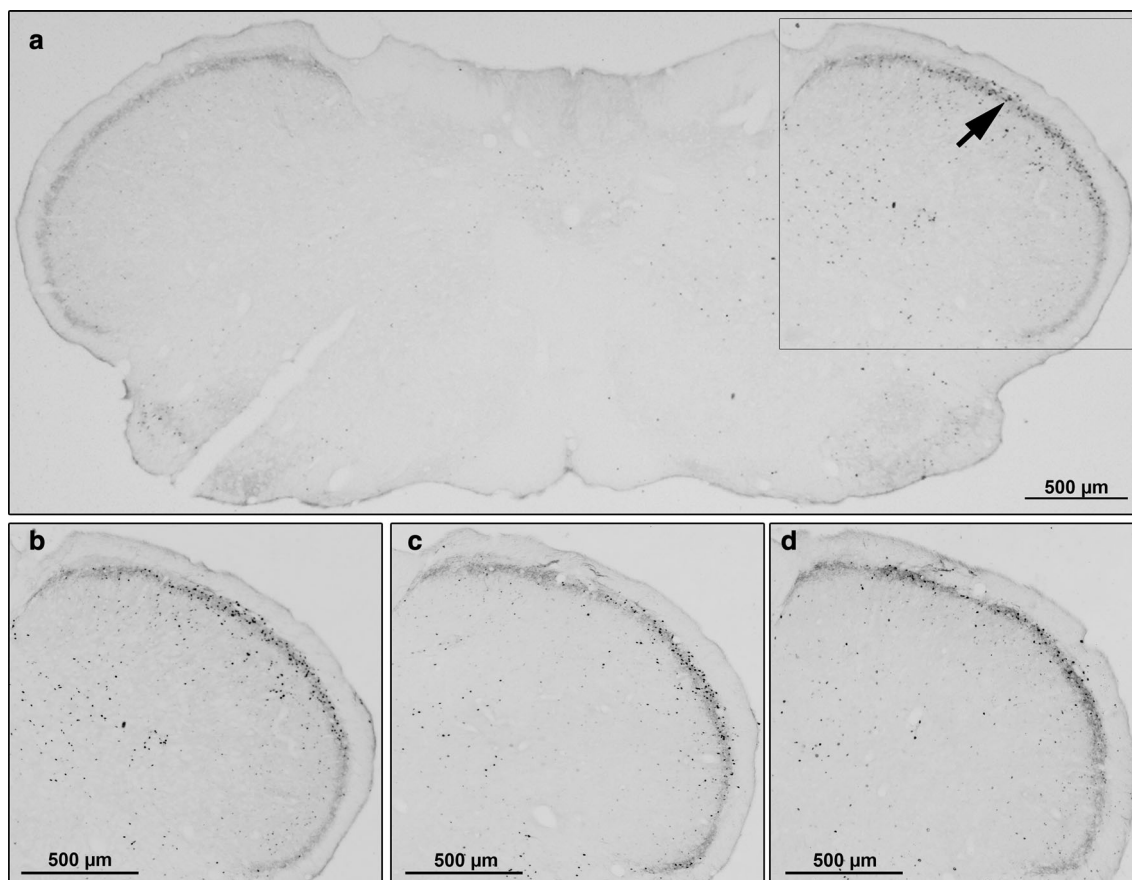
Fig. 5 Representative histological images following c-Fos immunostaining in Sprague–Dawley male rats. Subcutaneous formalin injection induced an increase in the number of c-Fos IR neurons on the ipsilateral side demonstrated on the transverse section of medulla containing the TNC from the control + formalin subgroup (**a**, **b**; contralateral side is indicated with an incision on the ventral side of the section). The pretreatments (KA-1: **c**; KA-2: **d**), reduced the amount of IR cells in the superficial layers of TNC as compared with control + formalin group (**b**). *Black arrow* c-Fos IR neurons in the superficial laminae; *black frame* magnified area, which can be seen in images **b–d**; *TNC* trigeminal nucleus pars caudalis, *IR* immunoreactive, *KA-1* N-(2-N,N-dimethylaminoethyl)-4-oxo-1H-quinoline-2-carboxamide hydrochloride, *KA-2* N-(2-N-pyrrolidinylethyl)-4-oxo-1H-quinoline-2-carboxamide hydrochloride

aspect of the mean number of c-Fos IR neurons, the treatments, preferentially with KA-2, resulted in significant reductions in IR cell count at certain levels of the assessed region (the c-Fos changes followed the somatotopic representation of the trigeminal nociceptors in the injected whisker pad area; Strassman and Vos 1993). Besides the observed significant differences, the effects of the treatment are well demonstrated by the curves in Fig. 6.

HPLC measurements and pharmacokinetics

The concentrations of KYNA and KYNA amides measured in rat serum and CNS samples by HPLC are demonstrated in Table 1. The time-course profile of the KYNA amides in the rat serum revealed that after a steep increase in the concentration, a subsequent steep decrease occurred in the first hour, followed by a prolonged further gradual decrease (Fig. 7). Although the serum concentration of KA-2 did not show such a high level as that of KA-1, a slightly slower decrease

in concentration was observed. These observations are consistent with the calculated serum pharmacokinetic parameters (C_{max}, T_{max}, area under the curve (AUC_{0-t}), the half-life ($t_{1/2}$), apparent total clearance (CL/F_{obs}) and apparent volume of distribution (Vz/F_{obs})) of KA-1 and KA-2, demonstrated in Table 2. However, the increase in serum KYNA concentration following the i.p. injection of KA-2 was considerably higher (an approximately 200-fold maximal increase) as compared with that of KA-1 (an approximately 70-fold maximal increase), also well reflected by the above-mentioned pharmacokinetic parameters. To avoid the influence of the basal serum KYNA level on the calculated pharmacokinetic parameters, these basal concentrations were subtracted from the corresponding subsequent concentrations in the calculation of the pharmacokinetic parameters. The pharmacokinetic data therefore reflect only the KYNA amide-induced changes in KYNA concentrations. In the fifth hour, KA-1 and KA-2 were still present at 3.1 (0–61.5) μM and 0.5 (0.5–0.5) μM in the serum,
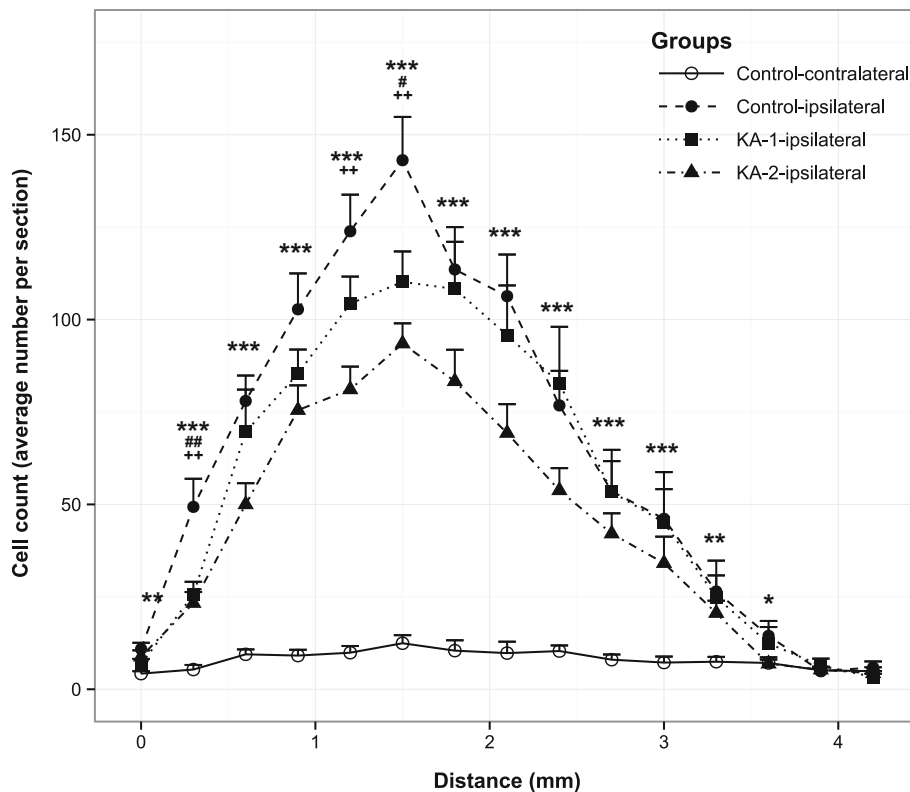
Fig. 6 The average number of c-Fos immunoreactive cells per section of TNC in Sprague–Dawley male rats after formalin injection with KYNA amide pretreatments. The distance was calculated caudally from the starting point of TNC. Subcutaneous formalin injection resulted in a higher number of c-Fos-IR neurones on the ipsilateral side compared with the contralateral side in the control + formalin group ($*p < 0.05$; $**p < 0.01$; $***p < 0.001$). The pretreatments (KA-1: $^{\#}p < 0.05$, $^{\#\#}p < 0.01$; KA-2: $^{++}p < 0.01$), reduced the amount of IR cells in the superficial layers of TNC as compared with the ipsilateral side in the control + formalin group. Sprague–Dawley male rats: $n = 9$–10 in each group; data are shown as mean ± SEM; *IR* immunoreactive, *TNC* trigeminal nucleus pars caudalis, *KA-1* N-(2-N,N-dimethylaminoethyl)-4-oxo-1H-quinoline-2-carboxamide hydrochloride, *KA-2* N-(2-N-pyrrolidinylethyl)-4-oxo-1H-quinoline-2-carboxamide hydrochloride

respectively, while the KYNA levels had approximately returned to the baseline level, preferentially in the case of KA-1 treatment. In the rat CNS samples, the KA-1 concentration was under LOD. However, KA-2 was present in detectable amounts in the CNS, reaching its maximum concentration (6.44 (5.62–7.85) pmol/g ww) after an hour which subsequently gradually decreased, but in the fifth hour it was still present at 1.98 (1.50–2.90) pmol/g ww. The CNS pharmacokinetics of KYNA following KA-1 and KA-2 administration showed quite similar profiles, characterized by an approximately maximal tenfold increase in basal concentration within the first hour. Vz/F_{obs} was relatively high in KA-1 and especially in KA-2. The apparent clearance was also high in the case of KA-2 relative to KA-1.

Discussion

Headache, one of the most common disorders of the nervous system, is a major health problem worldwide. The global prevalence for the adult population of active headache disorder is 46 % for headache in general, 11 % for migraine, 42 % for tension-type headache and 3 % for chronic daily headache (Stovner et al. 2007). The treatment of primary headache disorders is challenging requiring both acute and preventive therapeutic strategies (Weatherall 2015). The efficacy of these treatments is not always satisfactory and the contraindications and side effects often limit the options of the physician (Diener et al. 2015; Obermann et al. 2015). There is therefore a constant need to study and develop new molecules. In addition to the currently available drugs, e.g., NSAIDs, triptans, anticonvulsants, verapamil, propranolol, etc. (National Institute for Health and Care Excellence 2012), the pipeline of pharmaceutical research in this field involves the development of novel agents acting on the glutamatergic system due to its essential role in the nociceptive process (Dickenson et al. 1997; Diener et al. 2015). Animal and human studies have revealed that glutamate receptors are present in various parts of the trigeminal system (Quartu et al. 2002; Sahara et al. 1997; Tallaksen-Greene et al. 1992), and stimulation of the trigeminal nerve results in elevated

Table 1 The concentration of KYNA and KYNA amides in Sprague–Dawley male rat serum and CNS samples

Time (min)	Serum				CNS			
	KA-1 treatment		KA-2 treatment		KA-1 treatment		KA-2 treatment	
	KA-1 (µM)	KYNA (nM)	KA-2 (µM)	KYNA (nM)	KA-1 (pmol/g ww)	KYNA (pmol/g ww)	KA-2 (pmol/g ww)	KYNA (pmol/g ww)
0 (control)	0	75.7 (72.8–90.4)	0	75.7 (72.8–90.4)	0	5.33 (1.00–13.17)	0	5.33 (1.00–13.17)
15	87.4 (0–191.2)	5517.9 (3287.2–6290.1)	2.6 (2.2–20.9)	287.9 (239.1–6753.5)	<LOD	58.98 (53.37–277.22)	<LOD	17.41 (15.02–19.31)
30	35.6 (0–140.4)	1159.3 (523.8–2397.9)	20.9 (17.4–22.6)	16,709.5 (13,796.6–17,519)	<LOD	44.69 (29.43–104.13)	4.45 (3.88–4.67)	34.77 (25.01–50.53)
60	39.6 (0–114.4)	464.1 (304.9–1342.3)	13.7 (13.7–14)	3375.8 (3332.7–4604.1)	<LOD	58.61 (25.97–103.53)	6.44 (5.62–7.85)	65.70 (41.54–110.68)
120	19.5 (0–87.2)	561 (353.2–570.4)	3.2 (3–4.7)	334.6 (232.4–422.2)	<LOD	12.00 (11.07–15.68)	3.28 (2.75–3.31)	15.30 (10.81–18.47)
300	3.1 (0–61.5)	103.6 (99.1–128.2)	0.5 (0.5–0.5)	49.3 (110.3–150.1)	<LOD	13.73 (13.16–19.79)	1.98 (1.50–2.90)	22.43 (19.63–24.62)

The concentrations were measured with HPLC after pretreatment with KA-1 and KA-2. Sprague–Dawley male rats: $n = 5$ in each group; data are shown as median (interquartile range)

KYNA kynurenic acid, KA-1 N-(2-N,N-dimethylaminoethyl)-4-oxo-1H-quinoline-2-carboxamide hydrochloride, KA-2 N-(2-N-pyrrolidinylethyl)-4-oxo-1H-quinoline-2-carboxamide hydrochloride, LOD limit of detection

glutamate levels in the TNC (Oshinsky and Luo 2006). The peripheral application of glutamate to deep craniofacial tissue proved to be able to activate and sensitize nociceptive afferents and neurons in the upper cervical cord (Lam et al. 2009a, b). These findings suggest that excitatory amino acid receptors (and NMDA in particular) play an important role in pain processing and the sensitization process which is also present in migraineurs (Vikelis and Mitsikostas 2007). Ketamine, an NMDA antagonist, is so far the only promising treatment option for patients with severe or long-lasting migraine aura (Afridi et al. 2013). Another novel substance, tezampanel, which acts on the AMPA and kainate subtypes of ionotropic glutamate receptors (Alt et al. 2006), has also shown promising results in acute migraine therapy (Sang et al. 2004).

As regards the preclinical models of headache disorders, NTG is the most frequently used substance to trigger a delayed migraine-like attack (Sicuteri et al. 1987). Animal experiments have revealed that NTG can activate the trigeminal system and stimulate the second-order trigeminal neurons, which lead to increased c-Fos and neuronal nitric oxide synthase (nNOS) expression in the affected area (Párdutz et al. 2000; Tassorelli et al. 1997). NTG is also able to sensitize the trigeminal system in humans (Di Clemente et al. 2009). Together, these results confirm that NTG administration can model the central trigeminal nociceptor sensitization demonstrated in migraine patients (Burstein et al. 2000). With regard to the above-mentioned therapeutic strategy with the aim of neurotransmission modulation via the glutamatergic system, earlier studies revealed that KA-1 is able to attenuate the effects of NTG on the number of nNOS, calcium/calmodulin-dependent protein kinase II type alpha (CamKIIα) and calcitonin gene related peptide (CGRP) IR cells in the TNC, markers related to the activation and sensitization of the nociceptors (Vámos et al. 2010, 2009). KA-2 was later also tested in the NTG model and proved to be able to increase the KYNA concentration both in the C1–C2 region and in the serum. Pretreatment with KA-2 (0.5 and 1 mmol/kg) significantly reduced the effects of NTG on the CGRP-, c-Fos-, nNOS- and CaMKIIα-related changes in the C1–C2 region (Fejes-Szabó et al. 2014). To date, there has been only one study of the pharmacokinetic properties of KYNA amides, which found that only a small proportion of KA-1 decays into KYNA in the serum of C57B/6 mice (Zádori et al. 2011a).

In this study, we used another well-known model of trigeminal nociception, the orofacial formalin test. Formalin solution administered s.c. into the upper lip of rats causes tissue injury, inflammation and nociception (Clavelou et al. 1995). Immunohistochemical studies have revealed that formalin induces c-Fos and nNOS expression in the TNC, similarly as in the NTG model, which suggests

Fig. 7 The concentrations of KYNA and KYNA amides in serum and CNS samples of Sprague–Dawley male rats. **a**, **b** Concentrations of KYNA and KYNA amides in rat serum with the course of time after injection. **c**, **d** Concentrations of KYNA and KYNA amides in the CNS samples of the same animals. KA-1 concentrations were under the limit of detection in the CNS samples. Sprague–Dawley male rats: $n = 5$ in each group; data are shown as medians; *KYNA* kynurenic acid, *KA-1* N-(2-N,N-dimethylaminoethyl)-4-oxo-1H-quinoline-2-carboxamide hydrochloride, *KA-2* N-(2-N-pyrrolidinylethyl)-4-oxo-1H-quinoline-2-carboxamide hydrochloride
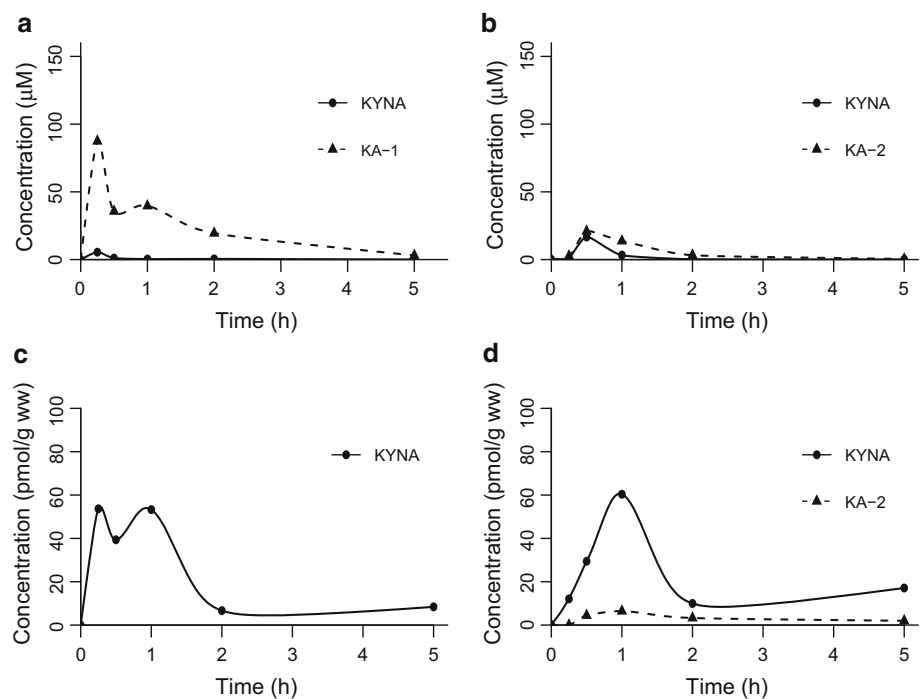
Table 2 Pharmacokinetic parameters of KYNA and KYNA amides in rat serum and CNS samples after intraperitoneal injection of KA-1 and KA-2

Serum					CNS				
Pharmacokinetic parameters	KA-1 treatment		KA-2 treatment		Pharmacokinetic parameters	KA-1 treatment		KA-2 treatment	
	KA-1	KYNA	KA-2	KYNA		KA-1	KYNA	KA-2	KYNA
$t_{1/2}$ (h)	1.09	0.91	0.84	0.64	$t_{1/2}$ (h)	NA	1.67	2.61	3.45
t_{max} (h)	0.25	0.25	0.50	0.50	t_{max} (h)	NA	0.25	1	1
C_{max} (μM)	87.44	5.44	20.87	16.63	C_{max} (pmol/g)	NA	53.66	6.44	60.37
AUC_{0-t} (μM h)	99.22	2.61	23.35	7.89	AUC_{0-t} (pmol/g h)	NA	86.46	16.24	97.77
Vz/F_{obs} ((μmol/kg)/(μmol/l))	15.17	–	50.02	–	Vz/F_{obs} ((pmol/kg)/(pmol/l))	NA	–	158,879.15	–
Cl/F_{obs} ((μmol/kg)/(μmol/l)/h)	9.61	–	41.81	–	Cl/F_{obs} ((pmol/kg)/(pmol/l)/h)	NA	–	42,220.03	–

The KYNA amides were applied in a dose of 1 mmol/kg. Sprague–Dawley male rats: $n = 5$ in each group

KYNA kynurenic acid, *KA-1* N-(2-N,N-dimethylaminoethyl)-4-oxo-1H-quinoline-2-carboxamide hydrochloride, *KA-2* N-(2-N-pyrrolidinylethyl)-4-oxo-1H-quinoline-2-carboxamide hydrochloride

the activation and sensitization of the area (Hunt et al. 1987; Párdutz et al. 2000). The behavioral effect of formalin is biphasic, with a short period of rubbing activity immediately after injection and then a tonic prolonged (20–22 min) second phase after a quiescent period (Raboisson and Dallel 2004). Using the formalin model, our aim was to compare the two compounds (KA-1 and KA-2) in an assessment method which involves both peripheral and central components of pain processing, with special interest in the pharmacokinetic explanation of the observed differences.

Our results indicated that KA-2 has more significant beneficial effects on the formalin-induced behavioral and immunohistochemical alterations. We carried out a comparative pharmacokinetic study to clarify this difference between the two analogs. With regard to the serum concentrations of the analogs following their i.p. administration, the levels of KA-2 were considerably lower than those of KA-1 from the aspects of peak concentration and AUC_{0-5h}. In contrast, KA-1 could not be detected in the examined CNS region, and the concentration of KA-2 was likewise relatively low. On the other hand, the serum pharmacokinetic data revealed that KA-2 decays into KYNA in larger amount as compared with KA-1, but nevertheless, in the examined CNS region, there is no major difference between KYNA levels following the treatments with KA-1 or KA-2. Summarizing these findings, the peak elevation of KYNA in the CNS

(approximately tenfold of the basal concentration) is considerably lower (by one order of magnitude) than that of peak elevation of KYNA in the serum (approximately 70–200-fold of the basal concentration) following the administration of KA-1 and KA-2, and with respect to CNS samples, there are no differences between KYNA levels. In view of these findings, the difference in the observed effects in behavioral and immunohistochemical studies could be explained by the differences in serum KYNA levels. From the aspect of a structure–activity relationship, the difference in peripheral conversion may stem from the structures of the two analogs, e.g., in the case of KA-2 the strained pyrrolidine moiety may influence the faster hydrolysis of the amide bond relative to the N,N-dimethyl function (KA-1). These findings suggest that the difference in the beneficial effects of the two analogs may be explained by the peripheral effect of elevated KYNA concentrations on formalin-induced pathological alterations. The molecular background would be the inhibition of NMDA receptor-mediated neurotransmission at the strychnine-insensitive glycine-binding site (Szalárdy et al. 2012) which is present on the peripheral process of the trigeminal nociceptors (Quartu et al. 2002; Watanabe et al. 1994). The observed peak serum KYNA concentration following KA-2 treatment during the experiment (16.71 μM) would be relevant with regard to the inhibition of glutamatergic neurotransmission via the above-mentioned possibility (Szalárdy et al. 2012).

In conclusion, our results draw attention to the role of influencing the glutamatergic system in the alleviation of peripheral sensitization, which can be utilized during future drug development. The possibility of targeting the peripheral component of pain processing would provide an option of pharmaceutical drug design without the obligation of good penetration through the BBB, but other pharmacokinetic parameters, such as solubility and clearance, must be kept in mind. The present results and previous preclinical findings indicate that the KYNA amides, via their probable direct effects (KA-1; Zádori et al. 2011a) or serving as prodrugs (KA-2 in the current pharmacokinetic study), would be promising drug candidates in neurological disorders, including those involving pain and headache, with a high socioeconomic burden.

Compliance with ethical standards

Conflict of interest The authors declare that there is no conflict of interest.

References

Afridi SK, Giffin NJ, Kaube H, Goadsby PJ (2013) A randomized controlled trial of intranasal ketamine in migraine with prolonged aura. Neurology 80:642–647. doi:10.1212/WNL.0b013e3182824e66

Alt A, Weiss B, Ogden AM, Li X, Gleason SD, Calligaro DO, Bleakman D, Witkin JM (2006) In vitro and in vivo studies in rats with LY293558 suggest AMPA/kainate receptor blockade as a novel potential mechanism for the therapeutic treatment of anxiety disorders. Psychopharmacology 185:240–247. doi:10.1007/s00213-005-0292-0

Bahn A, Ljubojevic M, Lorenz H, Schultz C, Ghebremedhin E, Ugele B, Sabolic I, Burckhardt G, Hagos Y (2005) Murine renal organic anion transporters mOAT1 and mOAT3 facilitate the transport of neuroactive tryptophan metabolites. Am J Physiol Cell Physiol 289:C1075–C1084. doi:10.1152/ajpcell.00619.2004

Burstein R, Cutrer MF, Yarnitsky D (2000) The development of cutaneous allodynia during a migraine attack clinical evidence for the sequential recruitment of spinal and supraspinal nociceptive neurons in migraine. Brain 123:1703–1709

Carpenter M, Sutin J (1983) Human neuroanatomy, 8th edn. Williams & Wilkins, Baltimore

Clavelou P, Dallel R, Orliaguet T, Woda A, Raboisson P (1995) The orofacial formalin test in rats: effects of different formalin concentrations. Pain 62:295–301

Cohen J (1988) Statistical power analysis for the behavioral sciences, 2nd edn. Lawrence Erlbaum Associates Inc, Hillsdale. ISBN 0-8058-0283-5

Di Clemente L, Coppola G, Magis D, Gérardy P-Y, Fumal A, De Pasqua V, Di Piero V, Schoenen J (2009) Nitroglycerin sensitises in healthy subjects CNS structures involved in migraine pathophysiology: evidence from a study of nociceptive blink reflexes and visual evoked potentials. Pain 144:156–161. doi:10.1016/j.pain.2009.04.018

Dickenson AH, Chapman V, Green GM (1997) The pharmacology of excitatory and inhibitory amino acid-mediated events in the transmission and modulation of pain in the spinal cord. Gen Pharmacol 28:633–638. doi:10.1016/S0306-3623(96)00359-X

Diener H-C, Charles A, Goadsby PJ, Holle D (2015) New therapeutic approaches for the prevention and treatment of migraine. Lancet Neurol 14:1010–1022. doi:10.1016/S1474-4422(15)00198-2

Fejes-Szabó A, Bohár Z, Vámos E, Nagy-Grócz G, Tar L, Veres G, Zádori D, Szentirmai M, Tajti J, Szatmári I, Fülöp F, Toldi J, Párdutz Á, Vécsei L (2014) Pre-treatment with new kynurenic acid amide dose-dependently prevents the nitroglycerine-induced neuronal activation and sensitization in cervical part of trigemino-cervical complex. J Neural Transm 121:725–738. doi:10.1007/s00702-013-1146-2

Fukui S, Schwarcz R, Rapoport SI, Takada Y, Smith QR (1991) Blood brain barrier transport of kynurenines: implications for brain synthesis and metabolism. J Neurochem 56:2007–2017. doi:10.1111/j.1471-4159.1991.tb03460.x

Fülöp F, Szatmári I, Vámos E, Zádori D, Toldi J, Vécsei L (2009) Syntheses, transformations and pharmaceutical applications of kynurenic acid derivatives. Curr Med Chem 16:4828–4842. doi:10.2174/092986709789909602

Gellért L, Fuzik J, Göblös A, Sárközi K, Marosi M, Kis Z, Farkas T, Szatmári I, Fülöp F, Vécsei L, Toldi J (2011) Neuroprotection with a new kynurenic acid analog in the four-vessel occlusion model of ischemia. Eur J Pharmacol 667:182–187. doi:10.1016/j.ejphar.2011.05.069

Gellért L, Varga D, Ruszka M, Toldi J, Farkas T, Szatmári I, Fülöp F, Vécsei L, Kis Z (2012) Behavioural studies with a newly

developed neuroprotective KYNA-amide. J Neural Transm 119:165–172. doi:10.1007/s00702-011-0692-8

Hervé C, Beyne P, Jamault H, Delacoux E (1996) Determination of tryptophan and its kynurenine pathway metabolites in human serum by high-performance liquid chromatography with simultaneous ultraviolet and fluorimetric detection. J Chromatogr B Biomed Appl 675:157–161

Hunt SP, Pini A, Evan G (1987) Induction of c-fos-like protein in spinal cord neurons following sensory stimulation. Nature 328:632–634. doi:10.1038/328632a0

ICH (1995) ICH harmonised tripartite guideline, validation of analytical procedures. Fed Regist 60:11260

Knyihár-Csillik E, Mihaly A, Krisztin-Peva B, Robotka H, Szatmari I, Fulop F, Toldi J, Csillik B, Vécsei L (2008) The kynurenate analog SZR-72 prevents the nitroglycerol-induced increase of c-fos immunoreactivity in the rat caudal trigeminal nucleus: comparative studies of the effects of SZR-72 and kynurenic acid. Neurosci Res 61:429–432. doi:10.1016/j.neures.2008.04.009

Lam DK, Sessle BJ, Hu JW (2009a) Glutamate and capsaicin effects on trigeminal nociception I: activation and peripheral sensitization of deep craniofacial nociceptive afferents. Brain Res 1251:130–139. doi:10.1016/j.brainres.2008.11.029.Glutamate

Lam DK, Sessle BJ, Hu JW (2009b) Glutamate and capsaicin effects on trigeminal nociception II: activation and central sensitization in brainstem neurons with deep craniofacial afferent input. Brain Res 1253:48–59. doi:10.1016/j.brainres.2008.11.056

Marosi M, Nagy D, Farkas T, Kis Z, Rózsa É, Robotka H, Fülöp F, Vécsei L, Toldi J (2010) A novel kynurenic acid analogue: a comparison with kynurenic acid. An in vitro electrophysiological study. J Neural Transm 117:183–188. doi:10.1007/s00702-009-0346-2

Nagy K, Plangár I, Tuka B, Gellért L, Varga D, Demeter I, Farkas T, Kis Z, Marosi M, Zádori D, Klivényi P, Fülöp F, Szatmári I, Vécsei L, Toldi J (2011) Synthesis and biological effects of some kynurenic acid analogs. Bioorg Med Chem 19:7590–7596. doi:10.1016/j.bmc.2011.10.029

Näsström J, Karlsson U, Post C (1992) Antinociceptive actions of different classes of excitatory amino acid receptor antagonists in mice. Eur J Pharmacol 212:21–29

National Institute for Health and Care Excellence (2012) Headaches in over 12 s: diagnosis and management. https://www.nice.org.uk

Obermann M, Holle D, Naegel S, Burmeister J, Diener H-C (2015) Pharmacotherapy options for cluster headache. Expert Opin Pharmacother 16:1177–1184. doi:10.1517/14656566.2015.1040392

Olesen J, Gustavsson A, Svensson M, Wittchen H-U, Jönsson B, on behalf of the CDBE2010 study group, the European Brain Council (2012) The economic cost of brain disorders in Europe. Eur J Neurol 19:155–162. doi:10.1111/j.1468-1331.2011.03590.x

Oshinsky ML, Luo J (2006) Neurochemistry of trigeminal activation in an animal model of migraine. Headache 46(Suppl 1):S39–S44

Párdutz Á, Krizbai I, Multon S, Vécsei L, Schoenen J (2000) Systemic nitroglycerin increases nNOS levels in rat trigeminal nucleus caudalis. Neuroreport 11:3071–3075. doi:10.1097/00001756-200009280-00008

Párdutz Á, Fejes A, Bohár Z, Tar L, Toldi J, Vécsei L (2012) Kynurenines and headache. J Neural Transm 119:285–296. doi:10.1007/s00702-011-0665-y

Paxinos G, Watson C (2007) The rat brain in stereotaxic coordinates, 6th edn. Elsevier, Amsterdam

Pereira EFR, Hilmas C, Santos MD, Alkondon M, Maelicke A, Albuquerque EX (2002) Unconventional ligands and modulators of nicotinic receptors. J Neurobiol 53:479–500. doi:10.1002/neu.10146

Quartu M, Serra MP, Ambu R, Lai ML, Del Fiacco M (2002) AMPA-type glutamate receptor subunits 2/3 in the human trigeminal sensory ganglion and subnucleus caudalis from prenatal ages to adulthood. Mech Ageing Dev 123:463–471

R Development Core Team (2002) The R Project for Statistical Computing. R Foundation for Statistical Computing

Raboisson P, Dallel R (2004) The orofacial formalin test. Neurosci Biobehav Rev 28:219–226. doi:10.1016/j.neubiorev.2003.12.003

Sahara Y, Noro N, Iida Y, Soma K, Nakamura Y (1997) Glutamate receptor subunits GluR5 and KA-2 are coexpressed in rat trigeminal ganglion neurons. J Neurosci 17:6611–6620

Sang CN, Ramadan NM, Wallihan RG, Chappell AS, Freitag FG, Smith TR, Silberstein SD, Johnson KW, Phebus LA, Bleakman D, Ornstein PL, Arnold B, Tepper SJ, Vandenhende F (2004) LY293558, a novel AMPA/GluR5 antagonist, is efficacious and well-tolerated in acute migraine. Cephalalgia 24:596–602. doi:10.1111/j.1468-2982.2004.00723.x

Schwarcz R (2004) The kynurenine pathway of tryptophan degradation as a drug target. Curr Opin Pharmacol 4:12–17. doi:10.1016/j.coph.2003.10.006

Sicuteri F, Bene E, Poggioni M, Bonazzi A (1987) Unmasking latent dysnociception in healthy subjects. Headache J Head Face Pain 27:180–185. doi:10.1111/j.1526-4610.1987.hed2704180.x

Stovner L, Hagen K, Jensen R, Katsarava Z, Lipton R, Scher A, Steiner T, Zwart J-A (2007) The global burden of headache: a documentation of headache prevalence and disability worldwide. Cephalalgia 27:193–210. doi:10.1111/j.1468-2982.2007.01288.x

Strassman AM, Vos BP (1993) Somatotopic and laminar organization of fos-like immunoreactivity in the medullary and upper cervical dorsal horn induced by noxious facial stimulation in the rat. J Comp Neurol 331:495–516. doi:10.1002/cne.903310406

Szalárdy L, Zádori D, Toldi J, Fülöp F, Klivényi P, Vécsei L (2012) Manipulating kynurenic acid levels in the brain—on the edge between neuroprotection and cognitive dysfunction. Curr Top Med Chem 12:1797–1806. doi:10.2174/156802612803989264

Tallaksen-Greene SJ, Young AB, Penney JB, Beitz AJ (1992) Excitatory amino acid binding sites in the trigeminal principal sensory and spinal trigeminal nuclei of the rat. Neurosci Lett 141:79–83

Tassorelli C, Joseph SA, Nappi G (1997) Neurochemical mechanisms of nitroglycerin-induced neuronal activation in rat brain: a pharmacological investigation. Neuropharmacology 36:1417–1424

Vámos E, Párdutz Á, Varga H, Bohár Z, Tajti J, Fülöp F, Toldi J, Vécsei L (2009) l-kynurenine combined with probenecid and the novel synthetic kynurenic acid derivative attenuate nitroglycerin-induced nNOS in the rat caudal trigeminal nucleus. Neuropharmacology 57:425–429. doi:10.1016/j.neuropharm.2009.06.033

Vámos E, Fejes A, Koch J, Tajti J, Fülöp F, Toldi J, Párdutz Á, Vécsei L (2010) Kynurenate derivative attenuates the nitroglycerin-induced camKIIα and CGRP expression changes. Headache 50:834–843. doi:10.1111/j.1526-4610.2009.01574.x

Vécsei L, Szalárdy L, Fülöp F, Toldi J (2013) Kynurenines in the CNS: recent advances and new questions. Nat Rev Drug Discov 12:64–82. doi:10.1038/nrd3793

Vikelis M, Mitsikostas DD (2007) The role of glutamate and its receptors in migraine. CNS Neurol Disord Drug Targets 6:251–257

Watanabe M, Mishina M, Inoue Y (1994) Distinct gene expression of the N-methyl-D-aspartate receptor channel subunit in peripheral neurons of the mouse sensory ganglia and adrenal gland. Neurosci Lett 165:183–186

Weatherall MW (2015) Drug therapy in headache. Clin Med 15:273–279

Zádori D, Ilisz I, Klivényi P, Szatmári I, Fülöp F, Toldi J, Vécsei L, Péter A (2011a) Time-course of kynurenic acid concentration in mouse serum following the administration of a novel kynurenic acid analog. J Pharm Biomed Anal 55:540–543. doi:10.1016/j.jpba.2011.02.014

Zádori D, Klivényi P, Plangár I, Toldi J, Vécsei L (2011b) Endogenous neuroprotection in chronic neurodegenerative disorders: with particular regard to the kynurenines. J Cell Mol Med 15:701–717. doi:10.1111/j.1582-4934.2010.01237.x

Zádori D, Nyiri G, Szonyi A, Szatmári I, Fülöp F, Toldi J, Freund TF, Vécsei L, Klivényi P (2011c) Neuroprotective effects of a novel kynurenic acid analogue in a transgenic mouse model of Huntington's disease. J Neural Transm 118:865–875. doi:10.1007/s00702-010-0573-6

Zhang Y, Huo M, Zhou J, Xie S (2010) PKSolver: an add-in program for pharmacokinetic and pharmacodynamic data analysis in Microsoft Excel. Comput Methods Programs Biomed 99:306–314. doi:10.1016/j.cmpb.2010.01.00